

Selectively Anchoring Pt Single Atoms at Hetero-interfaces of $\gamma\text{-Al}_2\text{O}_3/\text{NiS}$ to Promote Hydrogen Evolution Reaction

Yangyang Feng,^{1†} Yongxin Guan,^{1†} Huijuan Zhang¹, Zhengyong Huang¹, Jian Li¹, Zhiqiang Jiang,² Xiao Gu^{2*} and Yu Wang^{1*}

¹State Key Laboratory of Power Transmission Equipment and System Security, Chongqing University, 174 Shazheng Street, Shapingba District, Chongqing City, 400044, P.R. China.

²Department of Applied Physics Chongqing University 55 Daxuecheng South Road, Shapingba District Chongqing City 401331, P. R. China.

† These authors contributed equally to this work.

*Corresponding author wangy@cqu.edu.cn; gx@cqu.edu.cn

Materials and Methods

Materials:

The chemicals used in the experiments were directly used without purification: ammonium hydroxide ($\text{NH}_3 \cdot \text{H}_2\text{O}$, 28-30 wt%, J. T. Baker), ethylene glycol (99.99%, Fisher Chemical), sodium carbonate (Na_2CO_3 , 99.9%, Aldrich), aluminium nitrate ($\text{Al}(\text{NO}_3)_3$, 99.9%, Aldrich), nickel nitrate ($\text{Ni}(\text{NO}_3)_2$, 99.9%, Aldrich), nickel sulfate (NiSO_4 , 99.9%, Aldrich), sodium hydroxide (NaOH , 99.9%, Aldrich), sulfur powder (99.98%, Aldrich), chloroplatinic acid hexahydrate ($\text{H}_2\text{PtCl}_6 \cdot 6\text{H}_2\text{O}$, 37.50 wt% Pt, Aldrich).

Preparation of flower-like $\text{Ni}_2\text{Al}(\text{CO}_3)_2(\text{OH})_3$ nanosheets

15 mL $\text{NH}_3 \cdot \text{H}_2\text{O}$, 10 mL ethylene glycol, 5 mL $\text{Ni}(\text{NO}_3)_2$ (2 M), 2 mL $\text{Al}(\text{NO}_3)_3$ (2 M) and 7 mL Na_2CO_3 (1 M) were gradually added into beaker. Then stirred for 25 min until the mixture was turned into sapphire blue. And next, the mixture was poured into autoclave of 50 mL and put into an oven at 180 °C for 18 h. After reaction, the precursor was precipitated in the bottle and then washed several times separatively by DI water and ethanol. Finally, the precursor was dried in oven overnight.

Preparation of $\text{Pt}/\text{NiS@Al}_2\text{O}_3$

At first, the flower-like $\text{Ni}_2\text{Al}(\text{CO}_3)_2(\text{OH})_3$ nanoplates were put into the tube furnace and annealed at 750 °C for 200 min under H_2 atmosphere. After that, the $\text{Ni@Al}_2\text{O}_3$ was further annealed in Ar with sulfur under 350 °C for 100 min. After that, uniformly mix 100 mg $\text{NiS@Al}_2\text{O}_3$ with 0.57 ml chloroplatinic acid (~ 5.7 mg). Then, the mixture was calcined again in the tube furnace at 400 °C for 200 min under Ar atmosphere.

Preparation of porous $\gamma\text{-Al}_2\text{O}_3$ nanosheets

200 mg $\text{NiS@Al}_2\text{O}_3$ was dissolved in 30 mL 2 M hydrochloric acid for more than one day. The NiS nanoparticles were totally dissolved as $\gamma\text{-Al}_2\text{O}_3$ is pretty stable in acid. Finally weigh the left sample. The content of $\gamma\text{-Al}_2\text{O}_3$ is ~10 wt% calculated via the formula:

$$\gamma\text{-Al}_2\text{O}_3\% = M(\gamma\text{-Al}_2\text{O}_3)/M(\text{NiS@Al}_2\text{O}_3) \times 100\%$$

Where $M(\gamma\text{-Al}_2\text{O}_3)$ and $M(\text{NiS@Al}_2\text{O}_3)$ are the weight of $\gamma\text{-Al}_2\text{O}_3$ and $\text{NiS@Al}_2\text{O}_3$, respectively.

Preparation of Pt/NiS

Firstly, to prepare NiS nanoparticles, 9.8 mmol NiSO_4 , 9.8 mmol NaOH , 30 mL deionized water were mixed step by step under strong stirring. Then, after stirring for 15 min, the precursor solution changed into green solution. Subsequently, transfer the mixture into autoclave with a volume of 50 mL at 160 °C for 3 h. When the autoclave cooled naturally to room temperature in air, green samples were collected and washed by using deionized water and pure ethanol. After that, the as-prepared samples were dried in oven at 60 °C overnight to remove the absorbed water and ethanol. The dried samples were calcined in a tube furnace in H_2 at 750 °C for 200 min. Finally, the intermediate samples were annealed again with sulfur powders at 350 °C for 100 min in Ar. After that, Pt/NiS was prepared by the same procedure as preparation of $\text{Pt}/\text{NiS@Al}_2\text{O}_3$.

Characterization

Powder X-ray diffraction with $\text{Cu K}\alpha$ radiation (XRD, Bruker D8 Advance), field-emission scanning electron microscope (SEM) along with an energy dispersive spectrometer (EDS) analyzer (JSM-7800F, JEOL, 5 kV), transmission electron microscopy (TEM, FEI Tecnai G2 F30, 300 kV), high-angle annular dark field scanning transition electron microscopy (HAADF-STEM, FEI Titan Cubed Themis G2 300, 200 kV) X-ray absorption spectroscopy (XAS, SLAC National Accelerator Laboratory, 3 GeV), inductively coupled plasma atomic emission spectroscopy (ICP-

AES, iCAP 6300Duo), X-ray photo electron spectrometer with a monochromatic Al K α radiation (XPS, ESCALAB 250Xi, Thermo scientific, 225 W, 15 mA, 15 kV), Brunauer–Emmett–Teller surface area measurements (BET, Quantachrome Autosorb-6B surface-area and pore-size analyzer).

Electrochemical measurements

The whole catalytic measurements were conducted on CHI660E workstation by a three-electrode setup, which includes carbon rod, saturated calomel electrode (SCE) and glassy carbon electrode (3 mm). The catalyst mixture consists of 4 mg catalyst, 0.3 mL ethanol solvent and 0.1 mL Nafion solution (0.5 wt%). Then, drop 4 μ L suspension on the GCE and dried naturally. The mass loading of the electrode is \sim 0.57 mg/cm². Linear sweep voltammetry (LSV) was performed at the scan rates of 1, 2, 5 and 50 mV/s from -0.6 to 0 V in 0.5 M H₂SO₄ solution. The cyclic voltammetry (CV) was tested from 0 to 0.2 V at various scan rates of 10 to 120 mV/s. AC impedance tests were measured from 10⁵-0.1 Hz at various voltages. The potentials in the HER were vs. the reversible hydrogen electrode (RHE) based on the equation: E_(RHE) = E_(SCE) + 0.279 V in 0.5 M H₂SO₄ solution.

Computational details

All the computations were performed by using the generalized gradient approximation (GGA) with the Perdew-Burke-Ernzerh (PBE)³¹ within the DFT framework as implemented in Vienna ab initio simulation package (VASP).³² The project-augmented wave (PAW) method was used to represent core-valence electron interaction.³³ The valence electronic states were expanded in plane wave basis sets within a cutoff energy of 500 eV. The force threshold for the optimization was set as 0.01 ev/ \AA .

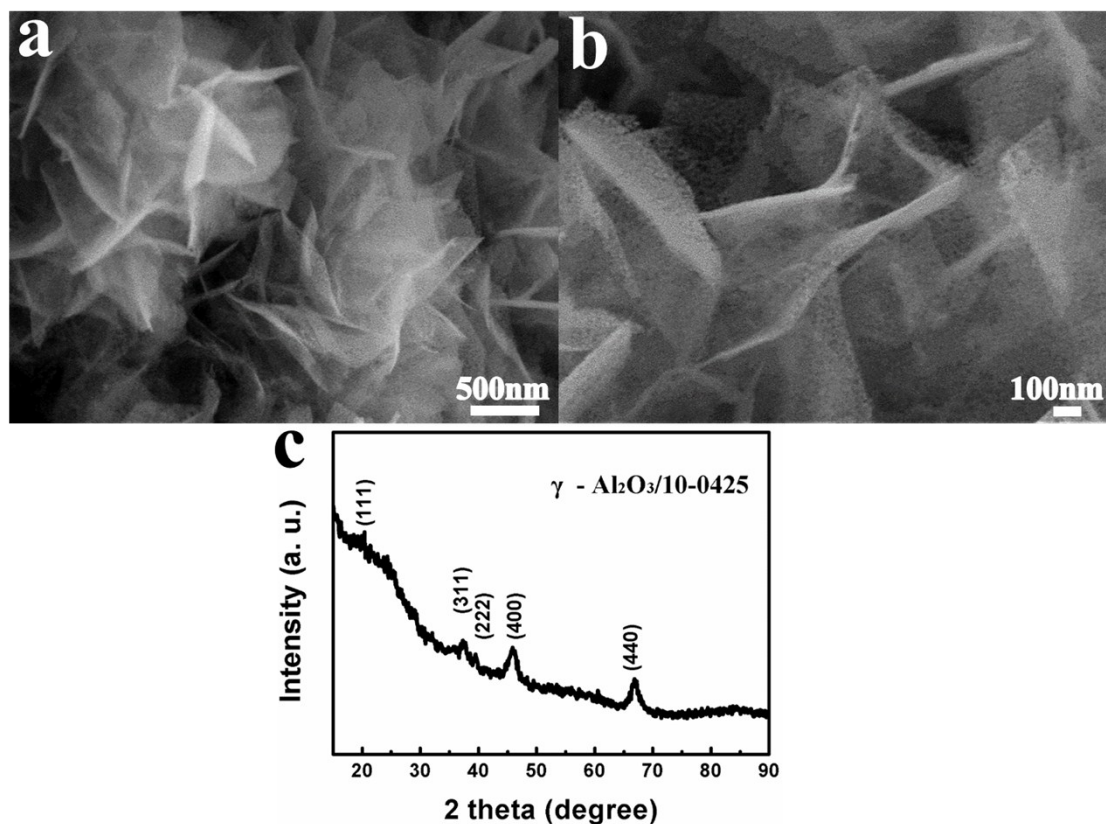


Figure S1 SEM images a - b and XRD pattern c of porous γ -Al₂O₃ nanosheets after dissolution by 2 M HCl.

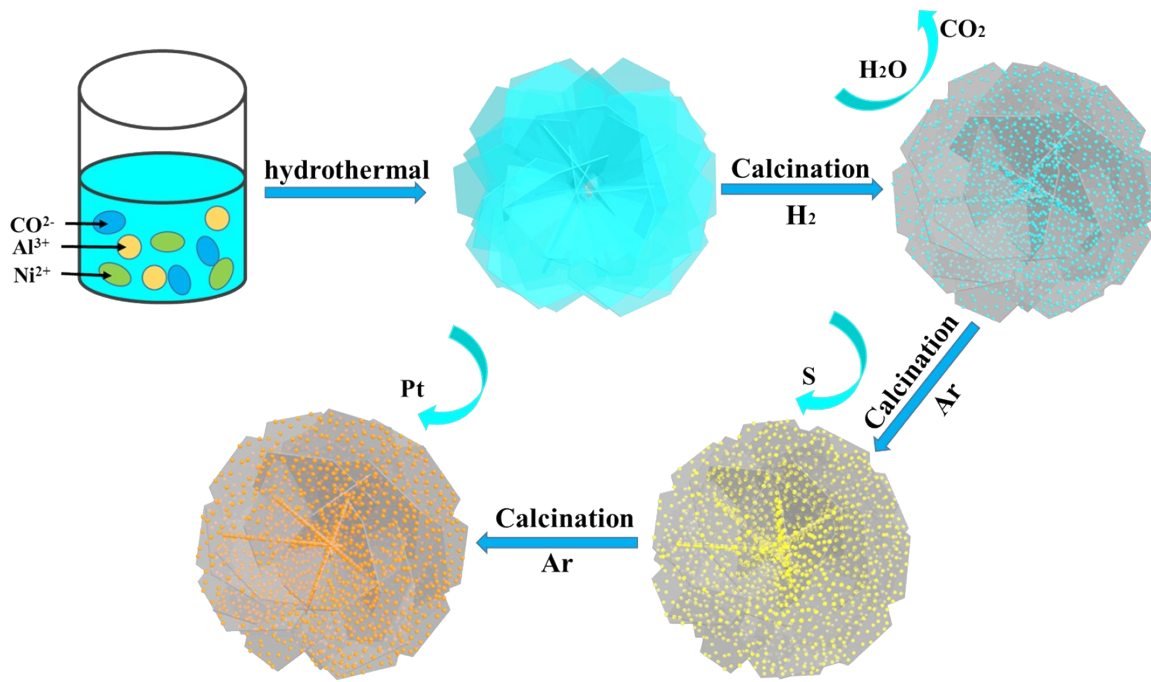


Figure S2 Schematic illustration to demonstrate the synthetic route from the precursor of three-dimensional $\text{Ni}_2\text{Al}(\text{CO}_3)_2(\text{OH})_3$ nanosheets to the intermediate products of $\text{Ni}@\text{Al}_2\text{O}_3$ and $\text{NiS}@\text{Al}_2\text{O}_3$, and finally to single Pt atoms anchored on $\text{NiS}@\text{Al}_2\text{O}_3$.

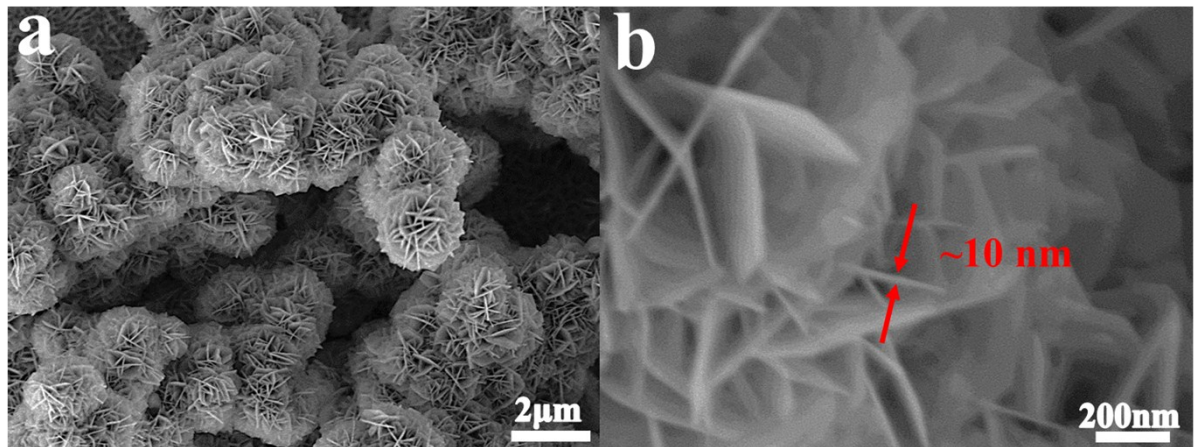


Figure S3 SEM images of the precursor of $\text{Ni}_2\text{Al}(\text{CO}_3)_2(\text{OH})_3$ nanosheets at different resolution.

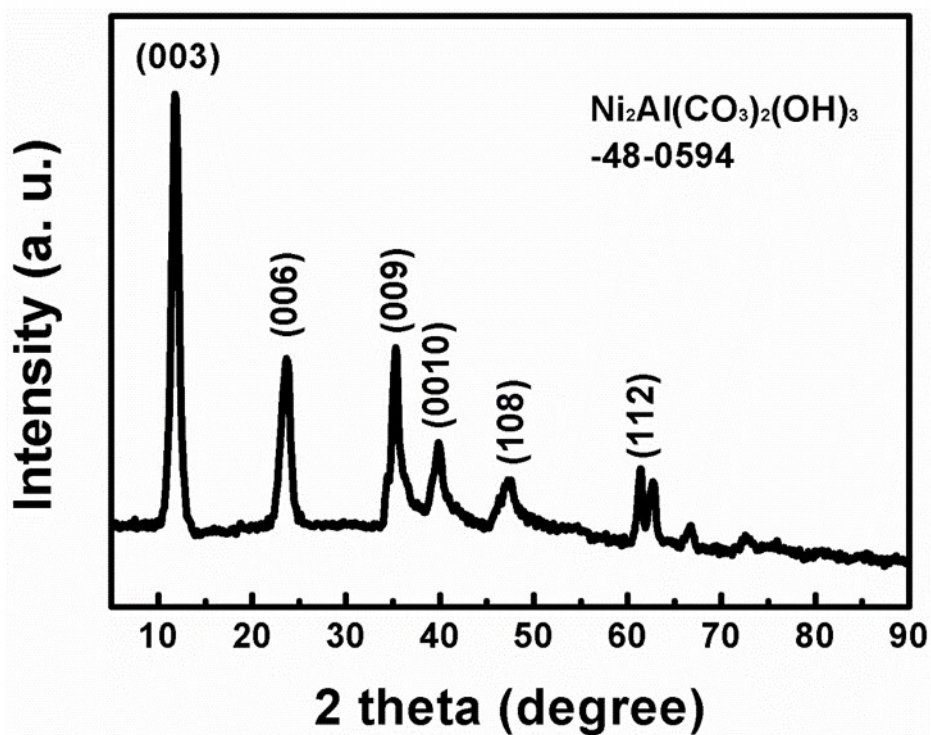


Figure S4 X-ray diffraction (XRD) pattern of $\text{Ni}_2\text{Al}(\text{CO}_3)_2(\text{OH})_3$ nanosheets.

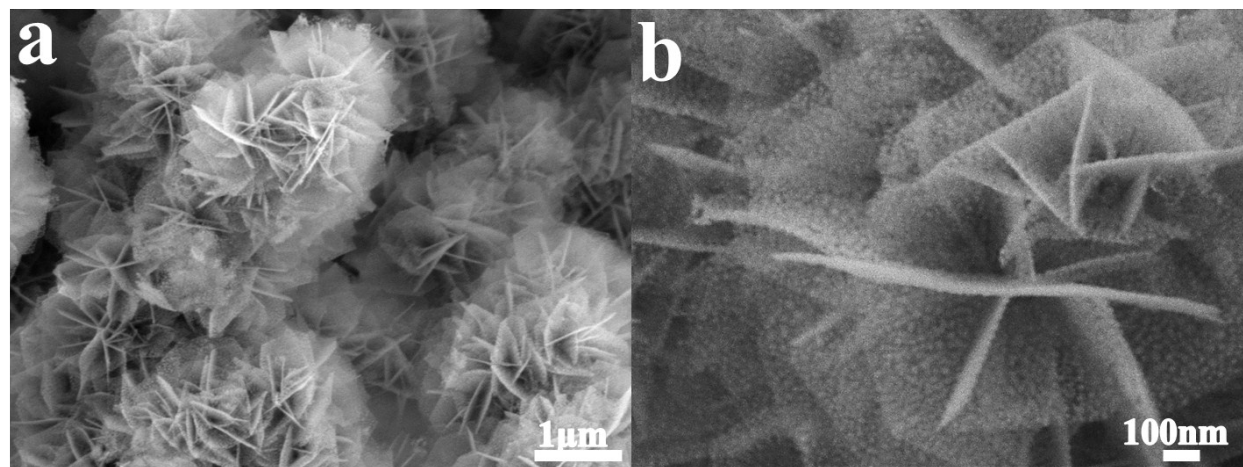


Figure S5 SEM images of the intermediate products of Ni@Al₂O₃ at different resolution.

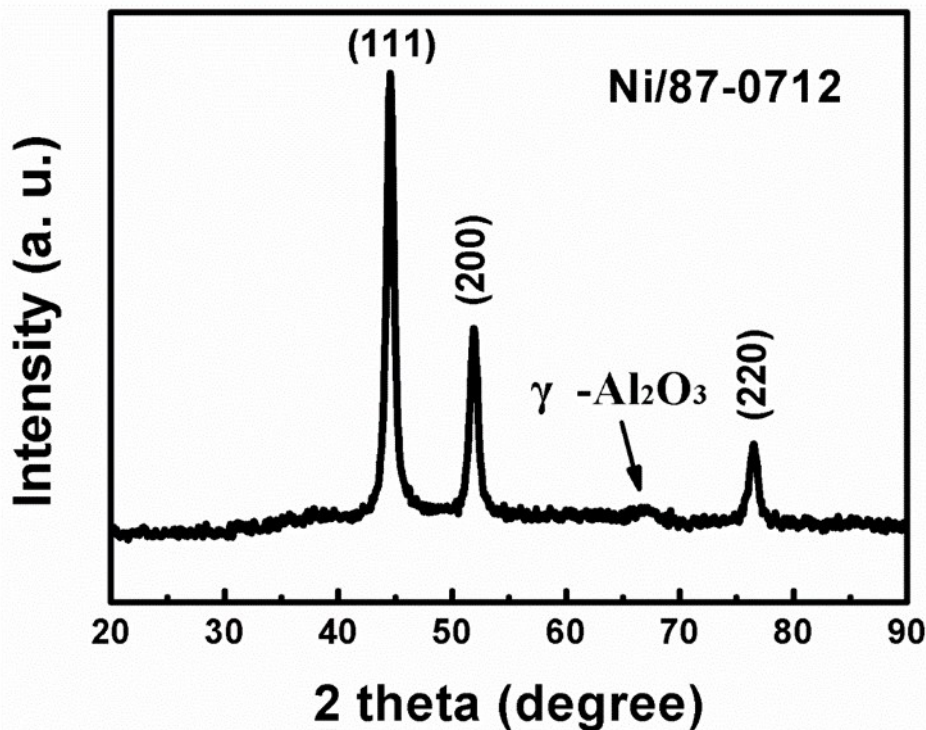


Figure S6 X-ray diffraction (XRD) pattern of Ni@Al₂O₃. Herein, a small peak at ~66.7° is observed, which is the feature peak of γ-Al₂O₃ (JCPDS No.10-0425).

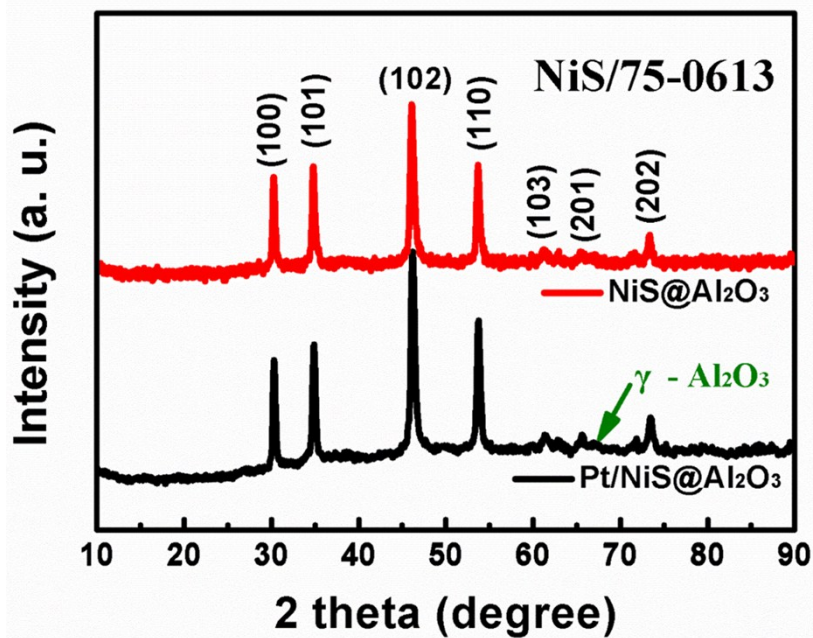


Figure S7 XRD patterns of Pt/NiS@Al₂O₃ and NiS@Al₂O₃. It indicates that Pt atom doping can hardly change the crystal structure of the NiS@Al₂O₃. Herein, a small peak at 66.7° is discovered, which is the characteristic peak of γ -Al₂O₃ (JCPDS No. 10-0425), referring to the γ -Al₂O₃ nanosheets anchoring Ni nanoparticles.

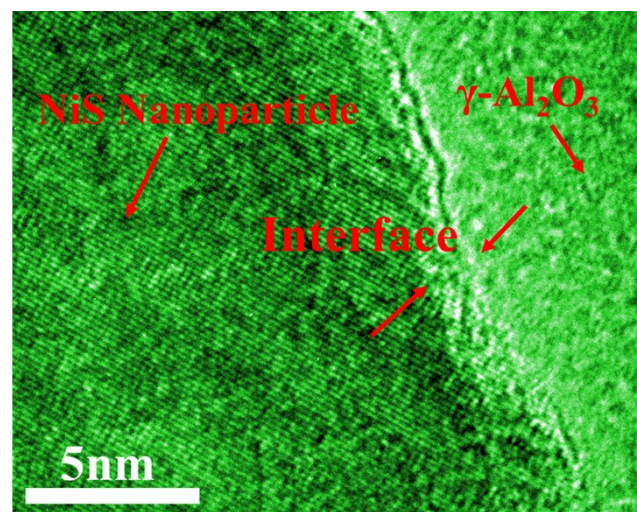


Figure S8 The HRTEM image of NiS@Al₂O₃.

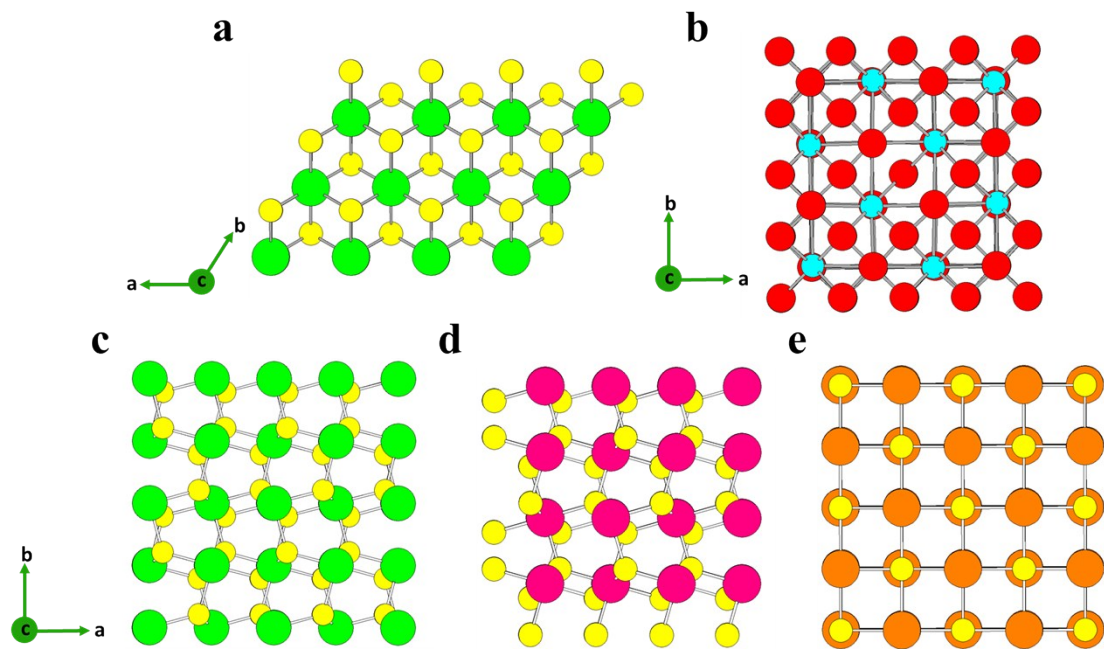


Figure S9 One possible contact crystal face of a NiS (001), c NiS₂ (001), d CoS₂ (001), e MnS₂ (001) and b γ -Al₂O₃ (001). NiS: crystal system: Hexagonal, $a=b=3.42$, $c=5.3$; NiS₂: crystal system: Hexagonal, $a=b=c=5.7$; CoS₂: crystal system: Hexagonal, $a=b=c=5.5$; MnS₂: crystal system: Hexagonal, $a=b=c=5.2$; γ -Al₂O₃: crystal system: Cubic, $a=b=c=7.9$. The green, pink, orange, yellow, red and blue balls denote nickel, cobalt, manganese, sulfur, aluminum and oxygen atoms, respectively. Owing to wide difference in crystal system and cell parameters, there are large crystal-lattice mismatch between TMS and γ -Al₂O₃.

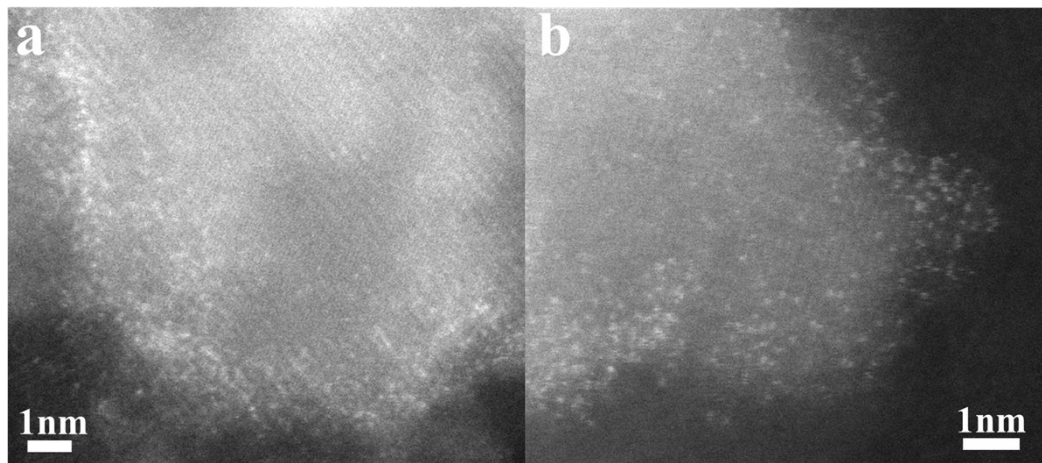


Figure S10 HAADF-STEM images of Pt/NiS@Al₂O₃ at the hetero-interfaces, in which we can see a large number of single atoms anchored on the interfaces, resulting from plenty of vacancy defects existing in interfaces owing to strong interaction between two different components. Furthermore, we can also detect many single Pt atoms anchored on NiS nanoparticles. The closer to the interface, the more Pt atoms anchored as there are more defects caused by strong interactions.

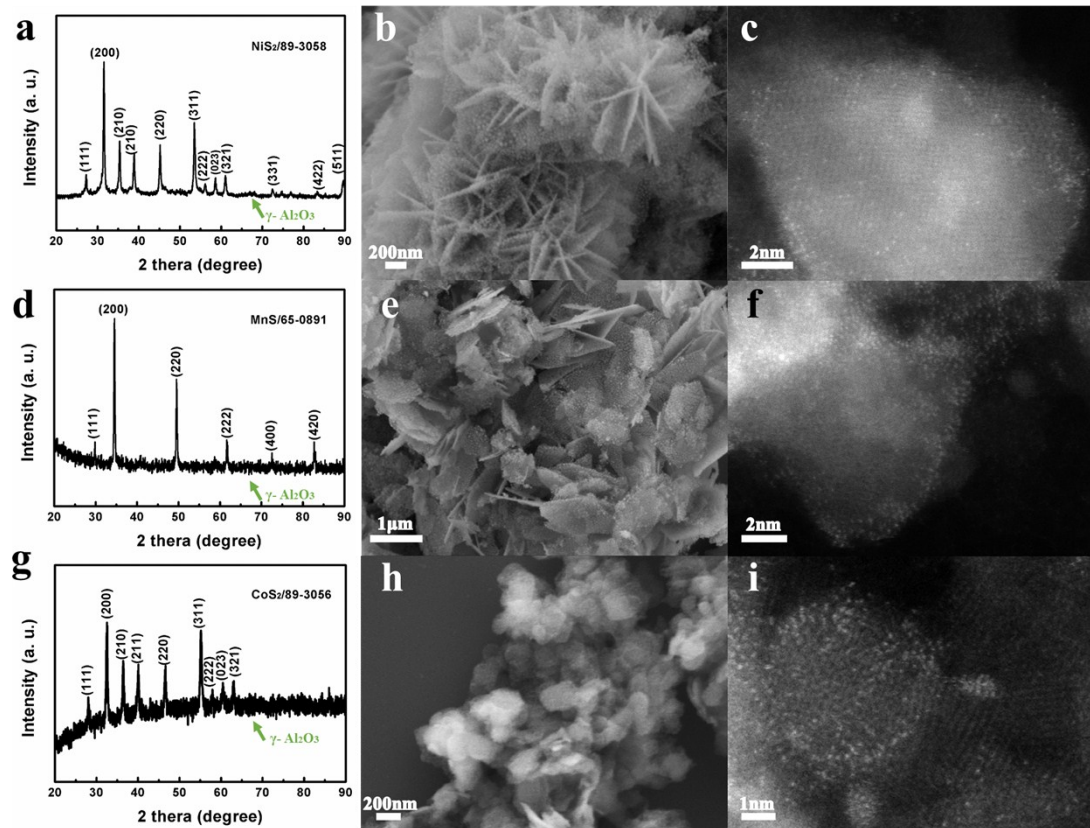


Figure S11 Typical characterizations of a-c Pt/NiS₂@Al₂O₃, d-f Pt/MnS@Al₂O₃, g-i Pt/CoS₂@Al₂O₃. a, d, g XRD patterns. b, e, h SEM images. c, f, i HAADF-STEM images.

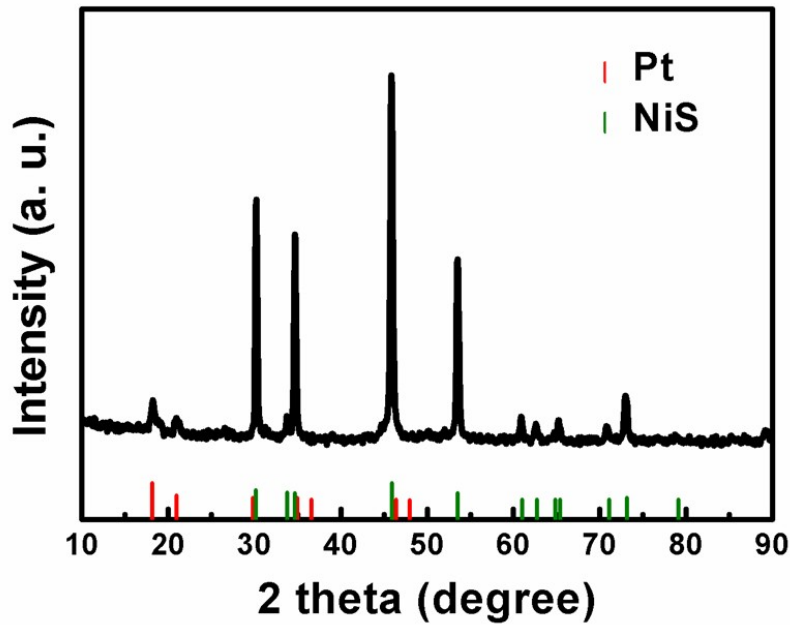


Figure S12 XRD pattern of Pt/NiS, in which metallic platinum peaks can be detected, indicating that Pt nanoparticles can be formed through the same conditions as Pt/NiS@Al₂O₃ with the similar Pt loading of ~2.8 %. It further suggests that heterostructure can effectively disperse Pt atoms and increase the loading amount of single-atom doping.

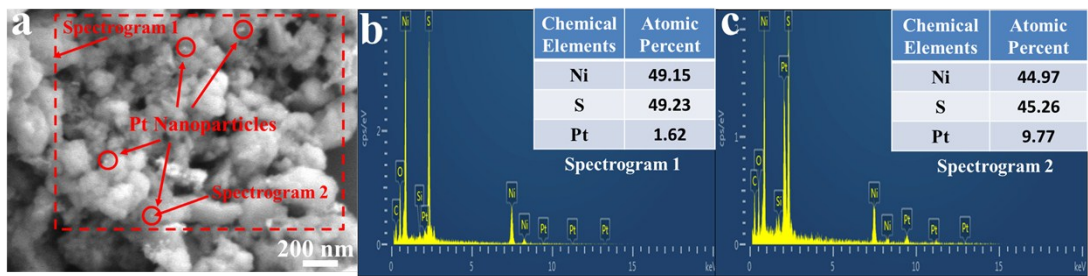


Figure S13 a SEM image of Pt anchored on pure NiS nanoparticles. b and c the corresponding EDS data of spectrogram 1 and 2 from local plane and point scanning, respectively. As observed, Pt nanoparticles can be formed when Pt anchored on pure NiS nanoparticles even through the same process as Pt/NiS@Al₂O₃. From the EDS data by point scanning on Pt nanoparticles, we can detect high atomic percent of Pt, further confirming that Pt nanoparticles exist in NiS nanoparticles. By comparison Pt/NiS@Al₂O₃ and NiS@Al₂O₃, we can find out NiS@Al₂O₃ heterostructure is more easily to anchor single Pt atoms due to plenty of vacancy defects derived from intense interaction between two different components.

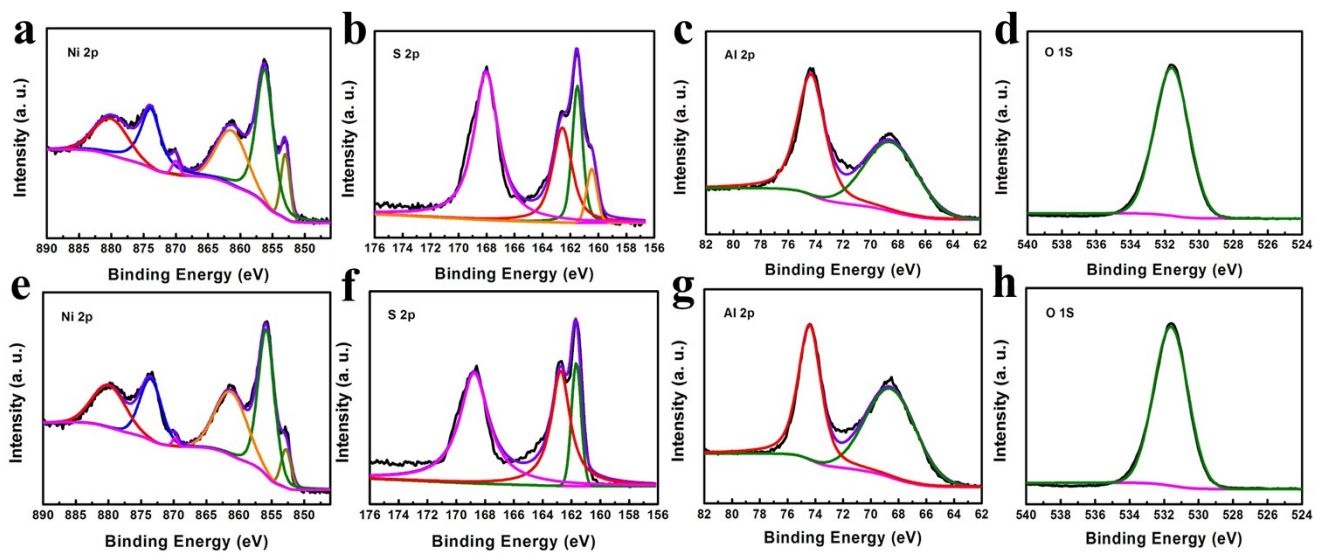


Figure S14 X-ray photoelectron spectroscopy (XPS) patterns of the major elements of Ni 2p, S 2p, Al 2p and O 1s in a-d Pt/NiS@Al₂O₃ and e-h NiS@Al₂O₃. In Fig. S14a and S14e, binding energies around 852.9 and 870.0 eV could be assigned to NiS, while the peaks at 856.2 and 874.0 eV as well as the two satellite peaks are corresponding to NiO in the surface.³⁴ The S 2p spectrum shows the peaks at 161.7 and 162.7 eV, which are originated from the 2p_{3/2} and 2p_{1/2} of S₂²⁻. And the satellite peaks at 168.8 eV, originated from the SO₄²⁺ species, indicates the partly oxidation of NiS on the surface. Herein, we can detect a small peak in Fig. S13b, which should be ascribed to Pt-S bond as there is only one difference between Pt/NiS@Al₂O₃ and NiS@Al₂O₃. In Al 2p and O 1s spectra, all the peaks show the similar binding energy of Al³⁺ and O²⁻, well matched with the previous literatures.^{35,36} These observations indicate that the Pt atoms are selectively anchored on NiS rather than γ-Al₂O₃.

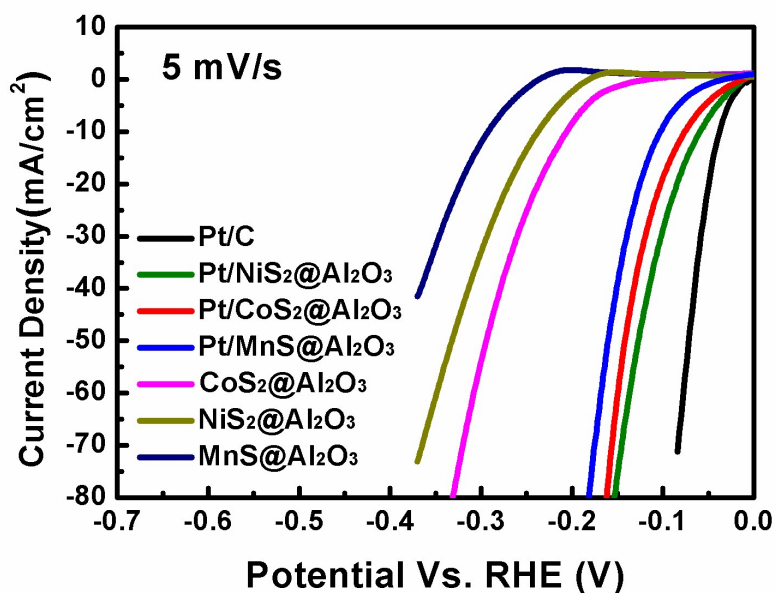


Figure S15 The linear sweep voltammetry (LSV) curves of Pt/C, Pt/NiS₂@Al₂O₃, Pt/CoS₂@Al₂O₃, Pt/MnS@Al₂O₃, NiS₂@Al₂O₃, CoS₂@Al₂O₃ and MnS@Al₂O₃ at the scan rate of 5 mV/s.

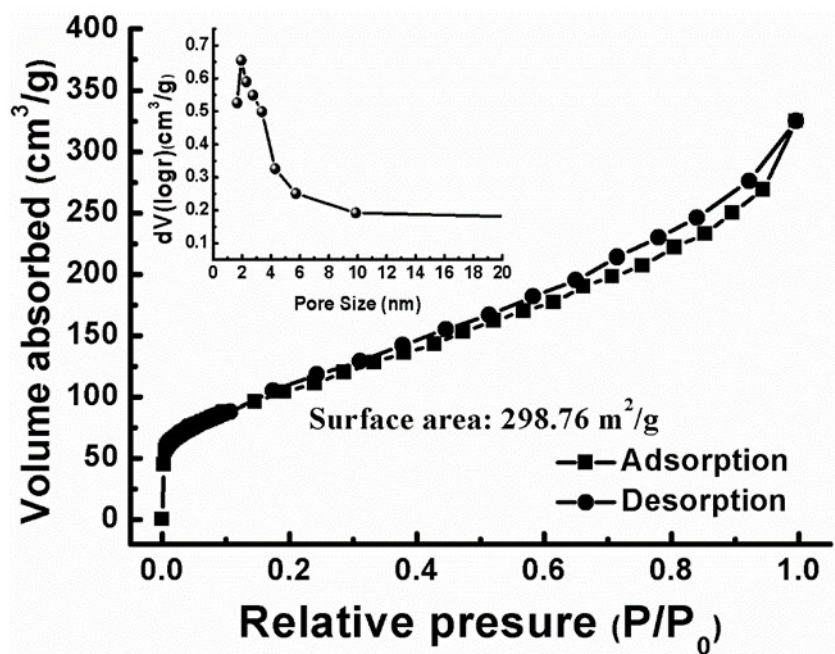


Figure S16 BET profile of Pt/NiS@Al₂O₃ to reveal the specific surface area and pore size distribution (inset) derived from the desorption branch.

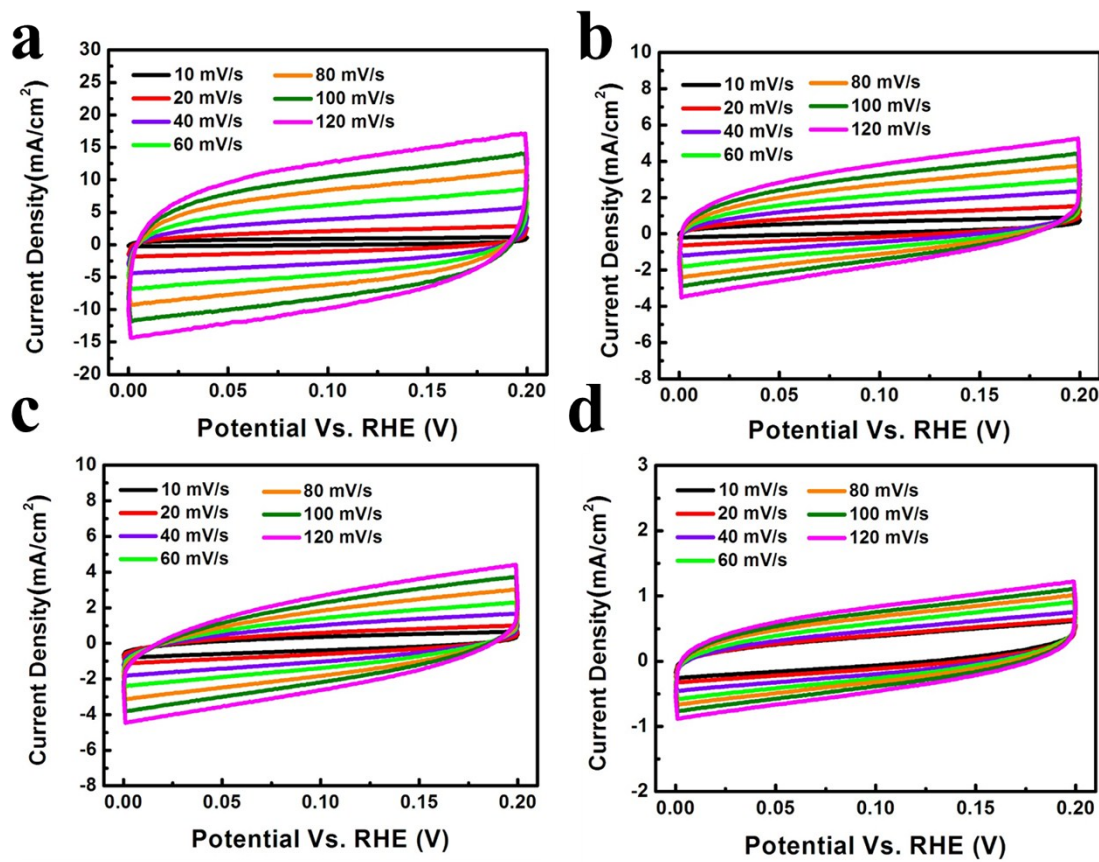


Figure S17 Cyclic Voltammograms (CV) of a Pt/NiS@Al₂O₃, b Pt/NiS, c NiS@Al₂O₃ and d NiS NP tested at various scan rates from 10 to 120 mV/s in the potential range of 0-0.2 V.

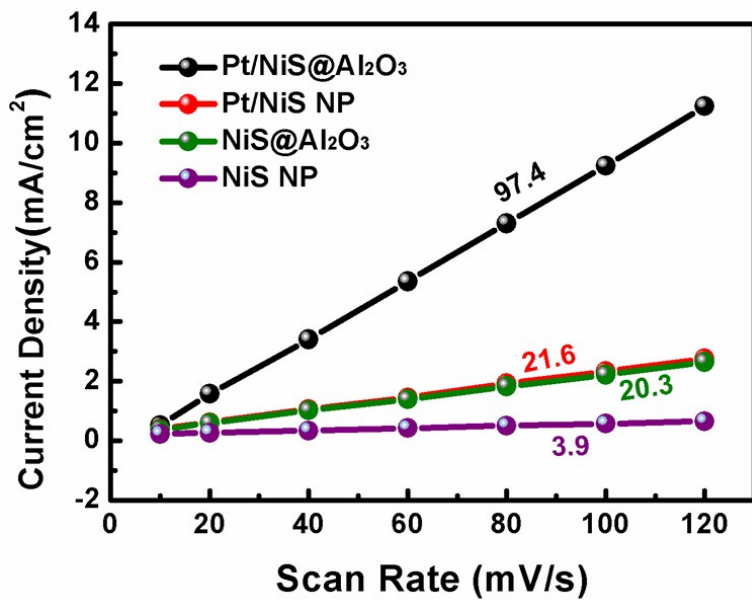


Figure S18 Scan rate dependence of the current densities of Pt/NiS@ Al_2O_3 , NiS@ Al_2O_3 , Pt/NiS and NiS NP.

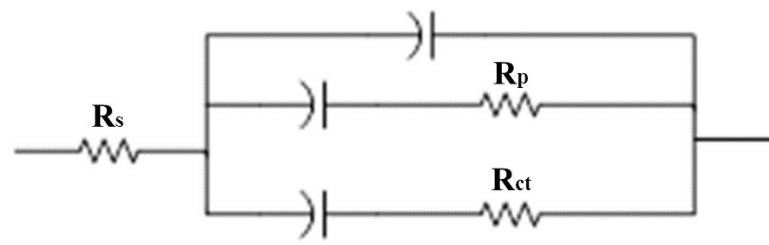


Figure S19 Equivalent circuit model for electrochemical impedance tests. R_s , R_p and R_{ct} represent electrolyte, electrode porosity and charge transfer resistance, respectively.

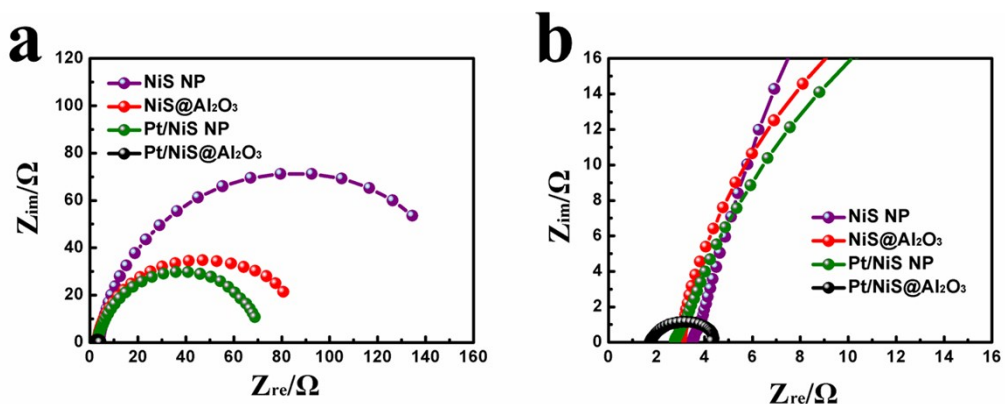


Figure S20 Nyquist plots of Pt/NiS@Al₂O₃, NiS@Al₂O₃, Pt/NiS and NiS NP tested at the same overpotential of 200 mV. b is the enlarged view of a.

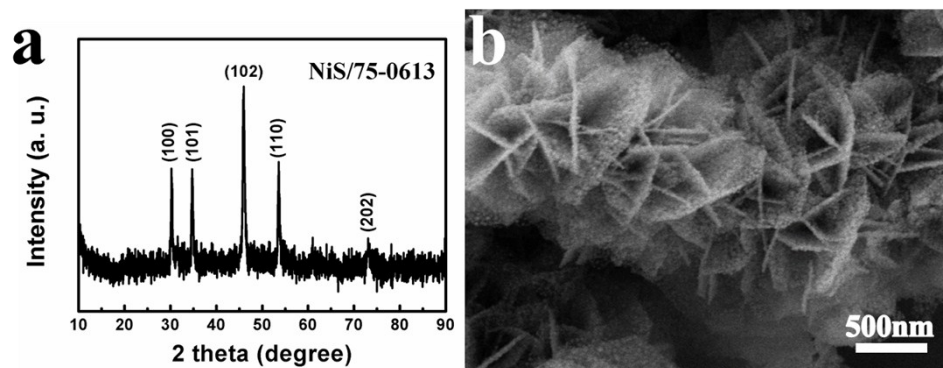


Figure S21 XRD and SEM image of Pt/NiS@Al₂O₃ after running for 120 h.

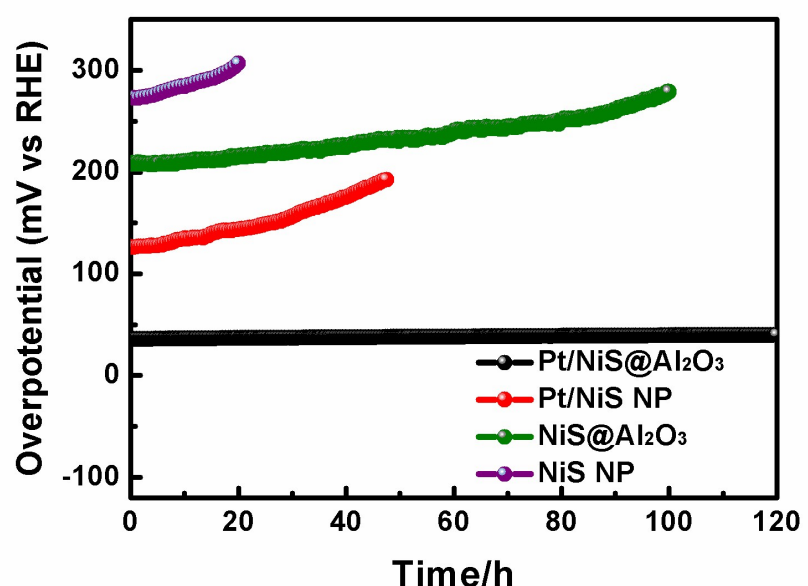


Figure S22 Durability tests of Pt/NiS@Al₂O₃, NiS@Al₂O₃, Pt/NiS and NiS NP for comparison.

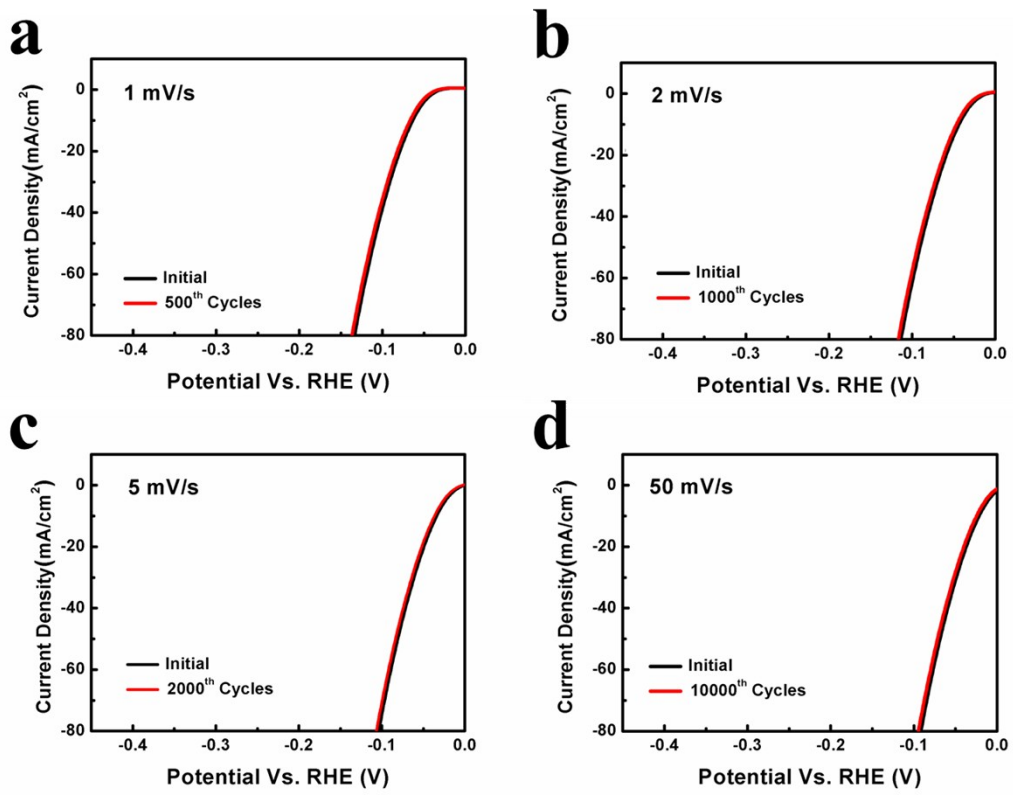


Figure S23 Polarization curves for Pt/NiS@Al₂O₃ tested at various scan rates of a 1 mV/s, b 2 mV/s, c 5 mV/s and d 50 mV/s in 0.5 M H₂SO₄.

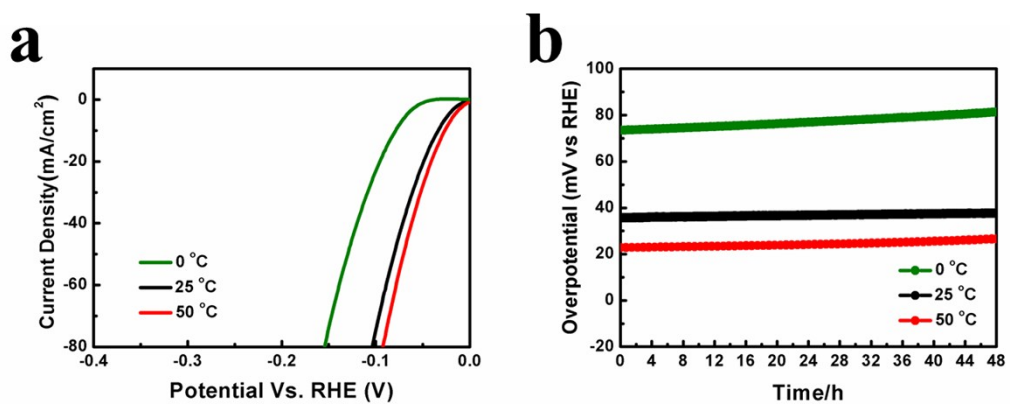


Figure S24 Temperature effect of Pt/NiS@Al₂O₃ tested in 0.5 M H₂SO₄. a Polarization curves tested at 0, 25 and 50 °C at a scan rate of 5 mV/s. b Durability test at 0, 25 and 50 °C at a constant current density of 10 mA/cm².

Composites	Molar ratio of Ni/S/Pt
NiS@Al₂O₃	989:1000:0
Pt/NiS@Al₂O₃	985:1000:15.4
NiS NPs	998:1000:0
Pt/NiS NPs	997:1000:14.5

Table S1 Inductively coupled plasma atomic emission spectroscopy (ICP-AES) tests of NiS@Al₂O₃, Pt/NiS@Al₂O₃, NiS NPs and Pt/NiS NPs, from which we can see Ni cations in NiS@Al₂O₃ is lower than S anions, indicating that Ni vacancies are formed through large crystal-lattice mismatch of NiS and γ-Al₂O₃.

Sample	Weight	Atom Ratio	Ref
Pt/NiS@Al₂O₃	2.8 %	1.5 %	This work
Pt/carbon	5.0 %	0.4 %	37
Pt/CeO₂-polyhedra	1.0 %	0.9 %	38
Pt/θ-Al₂O₃	0.18 %	0.09 %	39
Pt/Fe₃O₄	0.06 %	0.07 %	40
Pt/Fe	0.17 %	0.07 %	4
Pt/FeO_x	0.08 %	0.04 %	41
Pt/Fe	0.08%	0.03 %	42
Pt/g-C₃N₄	0.16 %	0.08 %	43
Pt/Graphene	1.52 %	0.09%	44
Pt/MoS₂	1.6 %	1.3 %	21
Pt/Mg(Sn)(Al)O	0.3 %	0.2 %	45
Pt/TiN	0.35 %	0.11 %	15
Pt/carbon	0.4 %	0.03 %	46
Pt/Mo₂C	0.2 %	0.2 %	2
Ag/CN	1 %	0.24 %	47
Au/CeO₂	0.05 %	0.04 %	48
Au/FeO_x	0.03 %	0.02 %	49
Au/MoS₂	0.7 %	0.6 %	50
Au/TiO₂	1.0 %	0.4 %	51
Fe/Graphene	1.5 %	0.3 %	52
Ir/FeO_x	0.01 %		53
Pd/TiO₂	1.5 %	0.6 %	5
Ni/Graphene		0.38 %	54
Fe/CN	2.16 %	1.09 %	55
Fe/CN	0.9 %	0.5 %	56
Fe/CN	1.4 %	0.7 %	57
Co/Carbon	3.6 %	0.7 %	58
Zn/Carbon	0.30 %	0.06 %	59
Ru/CN	0.30 %	0.08 %	60
Ni/CN	1.53 %	0.7 %	61
Co/CN	0.4 %	0.2 %	62
Au/NiFe-LDH	0.4 %	0.2 %	63
Ni/NG	4 %	0.82 %	64
Pt/MoS₂	7.5 %	6.2 %	65
Au/TiO₂	0.25 %	0.11 %	66

Table S2 The loading content of single atom doping reported in the previous literature.

	Ev (eV)	Es (eV)
$\gamma\text{-Al}_2\text{O}_3$	12.02	9.16
NiS	0.10	0.93

Table S3 The Ni and Al vacancy formation energies (Ev) and Pt substituted energies (Es) of NiS and $\gamma\text{-Al}_2\text{O}_3$

Composites	Molar ratio of Ni/S/Pt
Pt/NiS@Al ₂ O ₃	985:1000:15.3

Table S4 ICP-AES test of Pt/NiS@Al₂O₃ after running for 120 h.

Catalyst	Electrolytes	Current Density	Overpotential	Tafel slope (mV/dec)	Stability	Ref
3D flower-like	0.5 M H ₂ SO ₄	10 mA/cm ²	34 mV	35	98% 120 h	This work
Pt/NiS@Al₂O₃		20 mA/cm ²	49 mV			
β-NiS	0.5 M H ₂ SO ₄	10 mA/cm ²	202 mV	/	/	67
NiS₂ nanoparticle	0.5 M H ₂ SO ₄	1 mA/cm ²	230 mV	48.8	/	68
Ni₃S₂ film on fluorine-doped tin oxide	0.5 M H ₂ SO ₄	10 mA/cm ²	213 mV	52	95% 100 h	69
		20 mA/cm ²	243 mV			
NiS₂ film	0.5 M H ₂ SO ₄	10 mA/cm ²	239 mV	41.6	/	70
NiS nanoparticle	0.5 M H ₂ SO ₄	10 mA/cm ²	257 mV	88	98% 20 h	71
NiS₂ nanosheets	0.5 M H ₂ SO ₄	10 mA/cm ²	240 mV	41	83% 24 h	72
NiS₂ nanosheets array on carbon cloth	1.0 M PBS	10 mA/cm ²	243 mV	69	89% 15 h	73
NiS nanoparticle	1 M KOH	10 mA/cm ²	149 mV	104	94% 15 h	
NiS₂ nanoparticle	1 M KOH	10 mA/cm ²	474 mV	124	98% 20 h	74
Ni₃S₂ nanoparticle	1 M KOH	10 mA/cm ²	454 mV	128	96% 20 h	74
		10 mA/cm ²	335 mV	97	95% 20 h	74

Table S5 HER activities of NiS_x-based materials reported in the previous literature.

	Adsorption sites	ΔG (eV)
NiS	Ni	-3.59
	S	-4.07
Pt_{ad}	Pt	-0.02
	S	0.06
Pt_{sub}	S	0.34

Table S6. The values of ΔG of H adsorbed at different adsorption sites for NiS and Pt anchored on NiS structures. Pt_{ad} refers to Pt adsorbed on the surface of NiS or replacing Ni on the outer layer. Pt_{sub} stands for Pt replacing Ni on the sub-outer layer.

References

- 2 L.L. Lin, W. Zhou, R. Gao, S.Y. Yao, X. Zhang, W.Q. Xu, S.J. Zheng, Z. Jiang, Q.L. Yu, Y.W. Li, C. Shi, X.D. Wen, D. Ma, *Nature*, 544 (2017) 80-+
- 4 B. Qiao, A. Wang, X. Yang, L.F. Allard, Z. Jiang, Y. Cui, J. Liu, J. Li, T. Zhang, *Nat. Chem.*, 3 (2011) 634-641
- 5 P.X. Liu, Y. Zhao, R.X. Qin, S.G. Mo, G.X. Chen, L. Gu, D.M. Chevrier, P. Zhang, Q. Guo, D.D. Zang, B.H. Wu, G. Fu, N.F. Zheng, *Science*, 352 (2016) 797-801.
- 15 S. Yang, J. Kim, Y.J. Tak, A. Soon, H. Lee, *Angew. Chem., Int. Ed.*, 55 (2016) 2058-2062.
- 21 J. Deng, H.B. Li, J.P. Xiao, Y.C. Tu, D.H. Deng, H.X. Yang, H.F. Tian, J.Q. Li, P.J. Ren, X.H. Bao, *Energy Environ. Sci.*, 8 (2015) 1594-1601.
- 31 J.P. Perdew, K. Burke, M. Ernzerhof, *Phys. Rev. Lett.*, 77 (1996) 3865-3868.
- 32 G. Kresse, D. Joubert, *Phys. Rev. B*, 59 (1999) 1758-1775.
- 33 P.E. Blochl, *Phys. Rev. B*, 50 (1994) 17953-17979.
- 34 M. Liu, Y. Chen, J. Su, J. Shi, X. Wang, L. Guo, *Nat. Energy*, 1 (2016) 16151.
- 35 B.M. Reddy, K.N. Rao, G.K. Reddy, A. Khan, S.E. Park, *J. Phys. Chem. C*, 111 (2007) 18751-18758.
- 36 K.-S. Park, A. Benayad, M.-S. Park, A. Yamada, S.-G. Doo, *Chem. Commun.*, 46 (2010) 2572-2574.
- 37 C.H. Choi, M. Kim, H.C. Kwon, S.J. Cho, S. Yun, H.T. Kim, K.J.J. Mayrhofer, H. Kim, M. Choi, *Nat. Commun.*, 7 (2016).
- 38 J. Jones, H.F. Xiong, A.T. Delariva, E.J. Peterson, H. Pham, S.R. Challa, G.S. Qi, S. Oh, M.H. Wiebenga, X.I.P. Hernandez, Y. Wang, A.K. Datye, *Science*, 353 (2016) 150-154.
- 39 M. Moses-DeBusk, M. Yoon, L.F. Allard, D.R. Mullins, Z.L. Wu, X.F. Yang, G. Veith, G.M. Stocks, C.K. Narula, *J. Am. Chem. Soc.*, 135 (2013) 12634-12645.
- 40 J. Lin, B.T. Qiao, N. Li, L. Li, X.C. Sun, J.Y. Liu, X.D. Wang, T. Zhang, *Chem. Commun.*, 51 (2015) 7911-7914.
- 41 H.S. Wei, X.Y. Liu, A.Q. Wang, L.L. Zhang, B.T. Qiao, X.F. Yang, Y.Q. Huang, S. Miao, J.Y. Liu, T. Zhang, *Nat. Commun.*, 5 (2014).
- 42 Y.T. Shi, C.Y. Zhao, H.S. Wei, J.H. Guo, S.X. Liang, A.Q. Wang, T. Zhang, J.Y. Liu, T.L. Ma, *Adv. Mater.*, 26 (2014) 8147-8153.
- 43 X.G. Li, W.T. Bi, L. Zhang, S. Tao, W.S. Chu, Q. Zhang, Y. Luo, C.Z. Wu, Y. Xie, *Adv.*

- Mater., 28 (2016) 2427-2431.
- 44 S.H. Sun, G.X. Zhang, N. Gauquelin, N. Chen, J.G. Zhou, S.L. Yang, W.F. Chen, X.B. Meng, D.S. Geng, M.N. Banis, R.Y. Li, S.Y. Ye, S. Knights, G.A. Botton, T.K. Sham, X.L. Sun, Sci. Rep., 3 (2013).
- 45 Y.R. Zhu, Z. An, J. He, J. Catal, 341 (2016) 44-54.
- 46 J. Liu, M.G. Jiao, L.L. Lu, H.M. Barkholtz, Y.P. Li, Y. Wang, L.H. Jiang, Z.J. Wu, D.J. Liu, L. Zhuang, C. Ma, J. Zeng, B.S. Zhang, D.S. Su, P. Song, W. Xing, W.L. Xu, Y. Wang, Z. Jiang, G.Q. Sun, Nat. Commun., 8 (2017).
- 47 Z.P. Chen, S. Pronkin, T.P. Fellinger, K. Kailasam, G. Vile, D. Albani, F. Krumeich, R. Leary, J. Barnard, J.M. Thomas, J. Perez-Ramirez, M. Antonietti, D. Dontsova, ACS Nano, 10 (2016) 3166-3175.
- 48 B.T. Qiao, J.X. Liu, Y.G. Wang, Q.Q. Lin, X.Y. Liu, A.Q. Wang, J. Li, T. Zhang, J.Y. Liu, ACS Catal., 5 (2015) 6249-6254.
- 49 B.T. Qiao, J.X. Liang, A.Q. Wang, C.Q. Xu, J. Li, T. Zhang, J.Y. Liu, Nano Res., 8 (2015) 2913-2924.
- 50 Y.C. Lin, D.O. Dumcenco, H.P. Komsa, Y. Niimi, A.V. Krasheninnikov, Y.S. Huang, K. Suenaga, Adv. Mater., 26 (2014) 2857-2861.
- 51 C.Y. Wang, M. Yang, M. Flytzani-Stephanopoulos, Aiche J, 62 (2016) 429-439.
- 52 D.H. Deng, X.Q. Chen, L. Yu, X. Wu, Q.F. Liu, Y. Liu, H.X. Yang, H.F. Tian, Y.F. Hu, P.P. Du, R. Si, J.H. Wang, X.J. Cui, H.B. Li, J.P. Xiao, T. Xu, J. Deng, F. Yang, P.N. Duchesne, P. Zhang, J.G. Zhou, L.T. Sun, J.Q. Li, X.L. Pan, X.H. Bao, Sci. Adv., 1 (2015).
- 53 J. Lin, A.Q. Wang, B.T. Qiao, X.Y. Liu, X.F. Yang, X.D. Wang, J.X. Liang, J.X. Li, J.Y. Liu, T. Zhang, J. Am. Chem. Soc., 135 (2013) 15314-15317.
- 54 H.J. Qiu, Y. Ito, W.T. Cong, Y.W. Tan, P. Liu, A. Hirata, T. Fujita, Z. Tang, M.W. Chen, Angew. Chem., Int. Ed. , 54 (2015) 14031-14035.
- 55 Y.J. Chen, S.F. Ji, Y.G. Wang, J.C. Dong, W.X. Chen, Z. Li, R.A. Shen, L.R. Zheng, Z.B. Zhuang, D.S. Wang, Y.D. Li, Angew. Chem., Int. Ed. , 56 (2017) 6937-6941.
- 56 M.L. Zhang, Y.G. Wang, W.X. Chen, J.C. Dong, L.R. Zheng, J. Luo, J.W. Wan, S.B. Tian, W.C. Cheong, D.S. Wang, Y.D. Li, J. Am. Chem. Soc., 139 (2017) 10976-10979.
- 57 W.G. Liu, L.L. Zhang, X. Liu, X.Y. Liu, X.F. Yang, S. Miao, W.T. Wang, A.Q. Wang, T. Zhang, J. Am. Chem. Soc., 139 (2017) 10790-10798.
- 58 W.G. Liu, L.L. Zhang, W.S. Yan, X.Y. Liu, X.F. Yang, S. Miao, W.T. Wang, A.Q. Wang, T. Zhang, Chem. Sci., 7 (2016) 5758-5764.
- 59 P. Song, M. Luo, X.Z. Liu, W. Xing, W.L. Xu, Z. Jiang, L. Gu, Adv. Funct. Mater., 27 (2017).
- 60 X. Wang, W.X. Chen, L. Zhang, T. Yao, W. Liu, Y. Lin, H.X. Ju, J.C. Dong, L.R. Zheng, W.S. Yan, X.S. Zheng, Z.J. Li, X.Q. Wang, J. Yang, D.S. He, Y. Wang, Z.X. Deng, Y.E. Wu, Y.D. Li, J. Am. Chem. Soc., 139 (2017) 9419-9422.
- 61 C.M. Zhao, X.Y. Dai, T. Yao, W.X. Chen, X.Q. Wang, J. Wang, J. Yang, S.Q. Wei, Y.E. Wu, Y.D. Li, J. Am. Chem. Soc., 139 (2017) 8078-8081.
62. W. Liu, L. L. Cao, W. R. Cheng, Y. J. Cao, X. K. Liu, W. Zhang, X. L. Mou, L. L. Jin, X. S. Zheng, W. Che, Q. H. Liu, T. Yao and S. Q. Wei, Angew Chem Int Edit, 2017, **56**, 9312-+.
63. J. F. Zhang, J. Y. Liu, L. F. Xi, Y. F. Yu, N. Chen, S. H. Sun, W. C. Wang, K. M. Lange and B. Zhang, J Am Chem Soc, 2018, **140**, 3876-3879.
64. H. B. Yang, S. F. Hung, S. Liu, K. D. Yuan, S. Miao, L. P. Zhang, X. Huang, H. Y. Wang,

- W. Z. Cai, R. Chen, J. J. Gao, X. F. Yang, W. Chen, Y. Q. Huang, H. M. Chen, C. M. Li, T. Zhang and B. Liu, *Nature Energy*, 2018, **3**, 140-147.
65. H. Li, L. Wang, Y. Dai, Z. Pu, Z. Lao, Y. Chen, M. Wang, X. Zheng, J. Zhu, W. Zhang, R. Si, C. Ma and J. Zeng, *Nat Nanotechnol*, 2018.
66. J. W. Wan, W. X. Chen, C. Y. Jia, L. R. Zheng, J. C. Dong, X. S. Zheng, Y. Wang, W. S. Yan, C. Chen, Q. Peng, D. S. Wang and Y. D. Li, *Advanced Materials*, 2018, **30**.
67. X. Long, G.X. Li, Z.L. Wang, H.Y. Zhu, T. Zhang, S. Xiao, W.Y. Guo, S.H. Yang, *J. Am. Chem. Soc.*, 137 (2015) 11900-11903.
68. M.S. Faber, M.A. Lukowski, Q. Ding, N.S. Kaiser, S. Jin, *J Phys. Chem. C*, 118 (2014) 21347-21356.
69. N. Jiang, L. Bogoev, M. Popova, S. Gul, J. Yano, Y.J. Sun, *J Mater. Chem. A*, 2 (2014) 19407-19414.
70. D.S. Kong, J.J. Cha, H.T. Wang, H.R. Lee, Y. Cui, *Energy Environ. Sci.*, 6 (2013) 3553-3558.
71. D.Y. Chung, J.W. Han, D.H. Lim, J.H. Jo, S.J. Yoo, H. Lee, Y.E. Sung, *Nanoscale*, 7 (2015) 5157-5163.
72. X.L. Wu, B. Yang, Z.J. Li, L.C. Lei, X.W. Zhang, *Rsc Adv.*, 5 (2015) 32976-32982.
73. C. Tang, Z.H. Pu, Q. Liu, A.M. Asiri, X.P. Sun, *Electrochim. Acta*, 153 (2015) 508-514.
74. N. Jiang, Q. Tang, M.L. Sheng, B. You, D.E. Jiang, Y.J. Sun, *Catal. Sci. Technol.*, 6 (2016) 1077-1084.